DYNAMIC BEHAVIOR OF PILE GROUPS

by

Amir M. Kaynia, Graduate Student, MIT and

Eduardo Kausel, Associate Professor, MIT

Introduction

The technique most commonly used for the analysis and design of piles is based on the theory of beams on elastic foundation. The principal merits of this technique are its simplicity and versatility, and the reasonableness of the results obtained when adequate values of the coefficient of subgrade reaction are used. Among the more rigorous and advanced schemes for pile analysis, one must mention the pioneering works of Poulos (7,8,9) and those of Banerjee (2,3), which were both based on the application of Mindlin's fundamental solution for a point load in the interior of a semi-infinite elastic solid. The results of the extensive studies by Poulos brought out, in a systematic fashion, the key elements of pile group behavior, such as dependence of pile group stiffness on spacing between piles, their rigidity and length, and the distribution of loads on the raft. Still lacking, however, were results on the behavior of pile groups subjected to dynamic loads.

The more recent research on the dynamic response of pile groups was stimulated mainly by demands in the nuclear power plant industry, and by developments in the offshore structures technology. While the earlier studies focussed primarily on the behavior of a single pile, using both rigorous and approximate methods, some results are available now for pile groups as well. The first papers on this subject were contributed by Wolf and his associates (11), using numerical methods, and by Nogami (5,6) using analytical methods. A considerable improvement was presented recently by Waas and Hartmann (10), who implemented a very efficient scheme for the computation of the Green's functions for ring loads in their analyses of a concentric arrangement of piles.

The objective of this paper is to present the results of a study on the behavior of pile groups embedded in a halfspace, subjected to
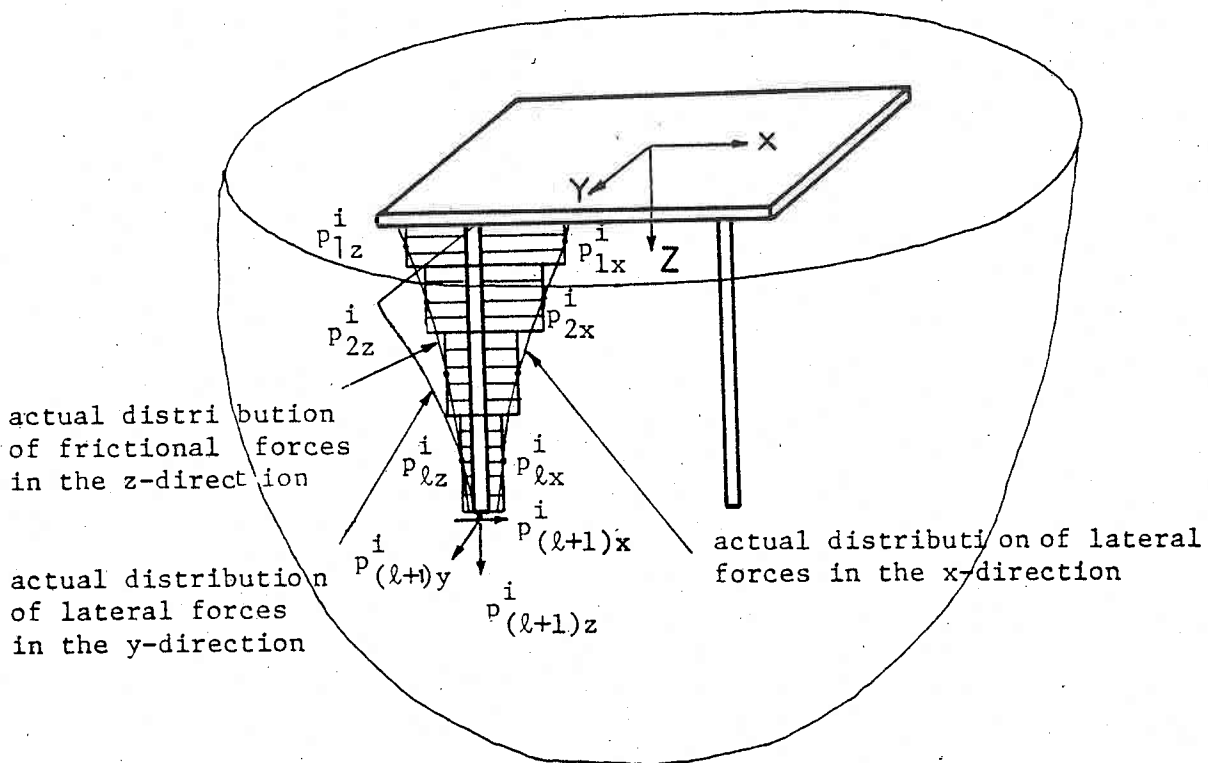
actual distribution
of frictional forces
in the z-direction

actual distribution
of lateral forces
in the y-direction

actual distribution of lateral
forces in the x-direction

Fig. 1 – Distribution of Forces on the
i^{th} pile of the group.

3

$$U_o^i = [u_{ox}^i \ \phi_{ox}^i \ u_{oy}^i \ \phi_{oy}^i \ u_{oz}^i \ u_{(\ell+1)x}^i \ \phi_{(\ell+1)x}^i \ u_{(\ell+1)y}^i \ \phi_{(\ell+1)y}^i \ u_{(\ell+1)z}^i]^T \quad (4)$$

Also, F_p^i is the dynamic flexibility matrix of the ith pile for fixed end conditions (i.e., the displacements observed at nodes 1 through $\ell+1$ produced by unit harmonic piecewise-constant segmental loads applied on a pile without soil, and with clamped ends. The entries in F_p^i corresponding to node $\ell+1$ are zero). Furthermore, ψ^i is the flexibility · matrix for unit harmonic end displacements or rotations (i.e., the displacements observed at the tip and center of the pile segments when the clamped ends of the otherwise free pile follow a prescribed harmonic motion). Neither F_p^i nor ψ^i incorporate interaction effects with the ground; these matrices can be obtained in closed form for any pile with constant properties.

If in addition one denotes the dynamic stiffness matrix of pile i by K_p^i (relating end forces with end displacement) and the vector of forces and moments at the two ends of this pile by P_o^i, that is

$$P_o^i = [R_{ox}^i \ M_{ox}^i \ R_{oy}^i \ M_{oy}^i \ R_{oz}^i \ R_{(\ell+1)x}^i \ M_{(\ell+1)x}^i \ R_{(\ell+1)y}^i \ M_{(\ell+1)y}^i \ R_{(\ell+1)z}^i]^T \quad (5)$$

Then one can write

$$P_o^i = K_p^i U_o^i + \psi^{i^T} p^i \quad (6)$$

The first term denotes the end forces due to prescribed end displacements U_o, and the second, the end forces (reactions) due to forces p^i acting on the pile.

Defining now the global load and displacement vectors for the N piles in the group:

$$P = \begin{Bmatrix} P^1 \\ P^2 \\ \vdots \\ P^N \end{Bmatrix} \quad ; \quad U = \begin{Bmatrix} U^1 \\ U^2 \\ \vdots \\ U^N \end{Bmatrix} \quad ; \quad P_o = \begin{Bmatrix} P_o^1 \\ P_o^2 \\ \vdots \\ P_o^N \end{Bmatrix} \quad ; \quad U_o = \begin{Bmatrix} U_o^1 \\ U_o^2 \\ \vdots \\ U_o^N \end{Bmatrix}$$

as well as the matrices

4

$$K_p = \left\{ \begin{array}{cccc} K_p^1 & & & \\ & K_p^2 & & \\ & & \ddots & \\ & & & K_p^N \end{array} \right\}$$

$$F_p = \left\{ \begin{array}{cccc} F_p^1 & & & \\ & F_p^2 & & \\ & & \ddots & \\ & & & F_p^N \end{array} \right\} \tag{7}$$

$$\psi = \left\{ \begin{array}{cccc} \psi^1 & & & \\ & \psi^2 & & \\ & & \ddots & \\ & & & \psi^N \end{array} \right\}$$

One can then write the following equations for the ensemble of piles in the group (compare with equations (3) and (6)):

$$U = \psi \, U_o - F_p \, P \tag{8a}$$

$$P_o = K_p \, U_o + \psi^T \, P \tag{8b}$$

Considering next the soil mass being acted upon by forces P (distributed uniformly over each segment), one can write

$$U = F_s \, P \tag{9}$$

where F_s is the soil flexibility matrix. Finally, combining eqs. (8) and (9) one gets

$$P_o = [K_p + \psi^T \, (F_s + F_p)^{-1} \psi] \, U_o = K_o \, U_o \tag{10}$$

The matrix K_o is a (10N x 10N) matrix that relates only the five components of forces at each end of the piles to their corresponding displacements. In other words, the degrees of freedom along the pile length have been condensed out without the need to form the complete stiffness matrix.

In order to obtain the dynamic stiffness of the pile group which is connected by a rigid plate, one needs to impose the appropriate geometric and force boundary conditions at the pile heads and pile tips (the boundary conditions at pile tips for floating piles are zero external forces at these points). Obviously, in the solution of equation (10) it is not necessary to perform the inversion indicated, but merely a triangular decomposition.

To obtain expressions for K_p, F_p and Ψ one has to solve the dynamic beam equation with the appropriate boundary conditions at the two ends (for details see ref. 4); to calculate F_s, an approach similar to that of Apsel's (1) has been used. In essence, Green's functions for buried dynamic barrel loads (distributed uniformly over the surface of a cylinder) were evaluated numerically by means of Fourier and Hankel transform techniques (for details, see ref. 4). The matrix F_s thus obtained corresponds to a soil without cavities (which will arise when the soil is drilled to provide room for the piles). The effect of the cavities is then accounted for explicitly in the formulation of the pile stiffness, subtracting the mass density and modulus of elasticity of the soil from those of the pile (ref. 4).

The extension of this model to the seismic analysis is achieved by decomposing the internal forces and displacements into the contributions of the "free field" motion and the "interaction" motion. This is equivalent to the use of substructuring techniques, the details of which are well known.

Pile Group Behavior

For the results presented here, it has been assumed that ν_s (Poisson ratio of the soil) = 0.40; ν_p (Poisson ratio of piles) = 0.25, L (length of piles) = 15d (d being the diameter of the piles), and ρ_s/ρ_p = 0.70, where ρ_s and ρ_p are the mass densities of the soil and piles, respectively. Also, pile heads were fixed to the cap.

a) Dynamic stiffnesses

The stiffness functions obtained by using the preceding formulation are complex quantities, which can be written as

$$K = k + i a_o c \qquad (11)$$

where $a_o = \omega d / C_s$ is the nondimensional frequency and C_s is the largest shear wave velocity of the soil profile. For horizontal and torsional cases, the dynamic stiffnesses were normalized with respect to the horizontal static stiffness of a single pile in the group, whereas for the vertical and rocking dynamic stiffnesses, the vertical static stiffness of a single pile has been used for normalization.

Fig. 2 shows the normalized horizontal and vertical stiffnesses of a 4 x 4 pile group in a halfspace for different pile spacings ($s/d = 2$, 5 and 10). For this case, $E_s/E_p = 10^{-3}$ (E_s and E_p are moduli of elasticity of the soil and piles, respectively).

These results show that the behavior of pile groups, for very close spacing and up to a certain frequency, is very similar to that of rigid footings; that is, k values decrease with frequency, and even become negative, which indicates a behavior dominated by inertia effects. On the other hand, interaction effects among the piles start to dominate the overall behavior of the group as frequency exceeds a certain limit. This can be verified by examining the changes in the patterns of k_{xx} and k_{zz} as s/d increases. Another interesting feature of these results is the very large interaction effect in the group; if there had been no interaction, the curves would have coincided with those of a single pile, the real part of which deviates only slightly from unity in the frequency range considered (dashed line). The large interaction effects are essentially due to the out-of-phase vibration of the piles. This point will be discussed again when the superposition scheme is examined later in this paper.

Fig. 3 shows the horizontal and vertical stiffnesses k and dampings c for a stiffer halfspace (or more flexible piles) ($E_s/E_p = 10^{-2}$) and for groups with different number of piles (2 x 2, 3 x 3 and 4 x 4 groups). For all these cases, s/d = 5. These figures display basically the same features of the case shown in Fig. 2 ($E_s/E_p = 10^{-3}$). However, the interaction effects seem to be less pronounced for the stiffer soil medium, as expected.

Another interesting feature of these results is that, for low frequencies, the radiation damping (as measured by the coefficients c_{xx} and c_{zz}) increase as the width of the foundation mat increases.

$$\frac{L}{d} = 15; \quad \frac{E_s}{E_p} = 10^{-3}; \quad \frac{\rho_s}{\rho_p} = 0.70$$
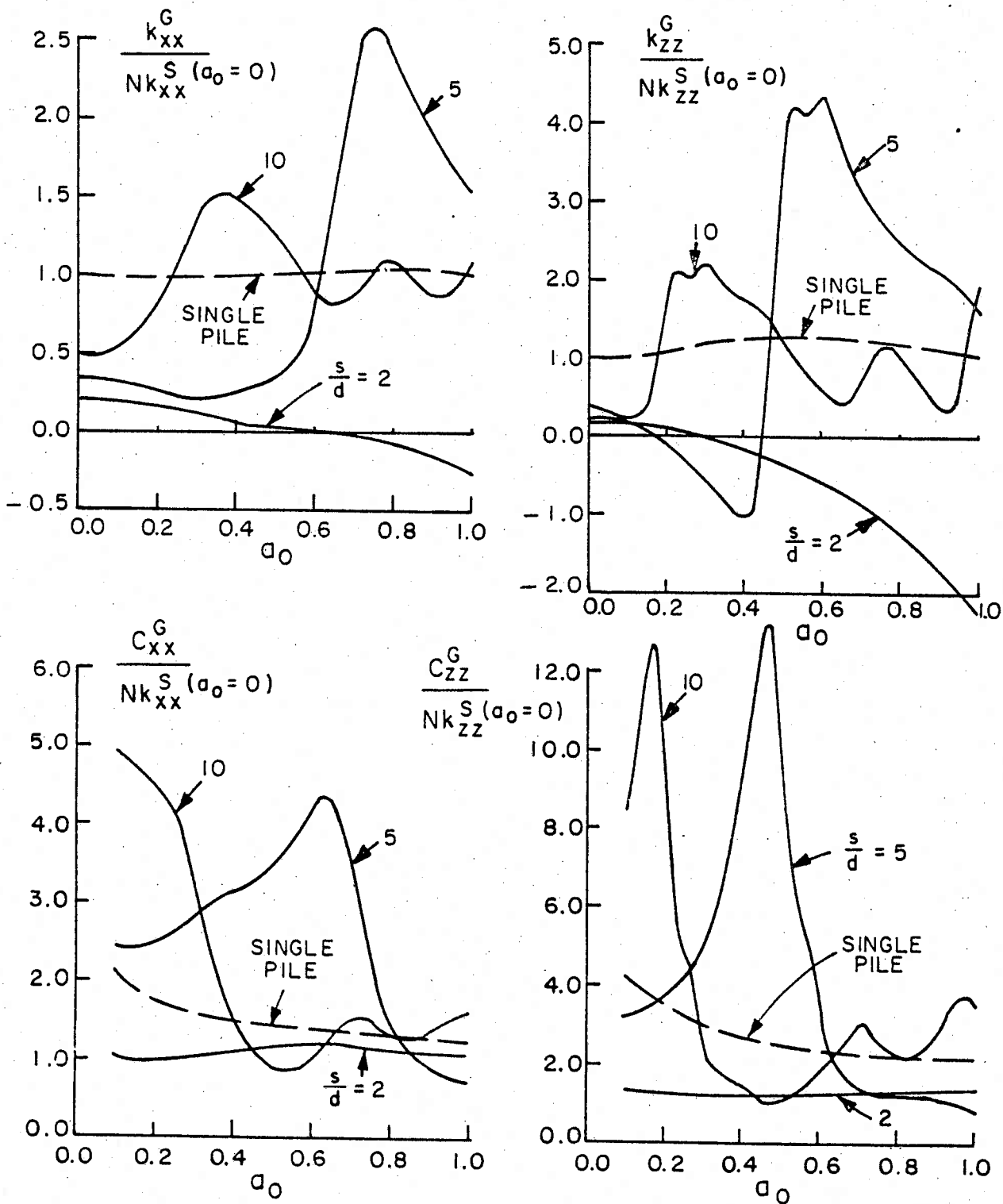

Fig. 2 - Horizontal and Vertical Dynamic Stiffnesses
for 4 x 4 pile groups.

$$\frac{L}{d} = 15 \; ; \quad \frac{s}{d} = 5 \; ; \quad \frac{E_s}{E_p} = 10^{-2} \; ; \quad \frac{\rho_s}{\rho_p} = 0.70$$
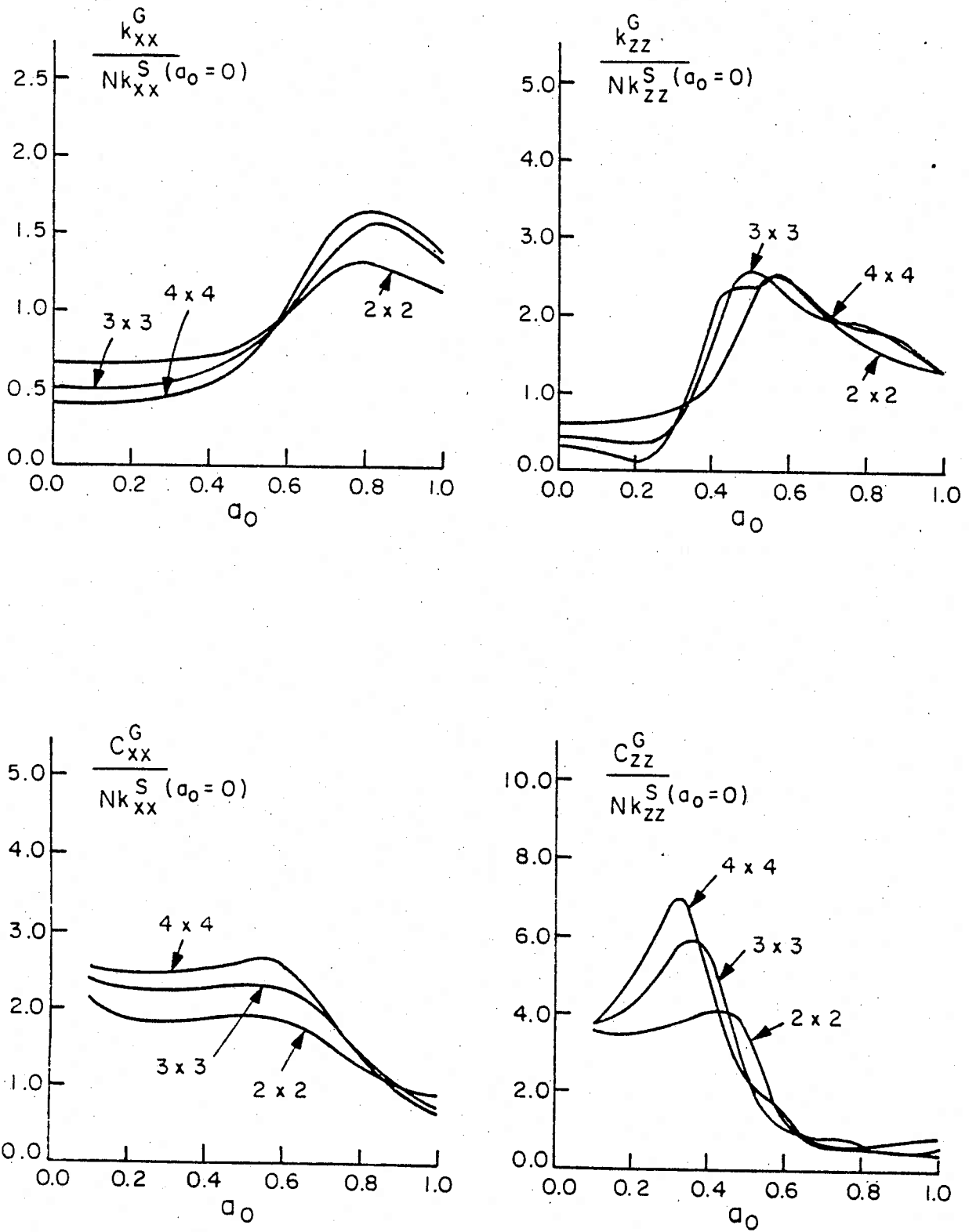

Fig. 3 - Horizontal and Vertical Dynamic Stiffnesses
for Pile Groups with s/d = 5.

Figs. 4 and 5 present the normalized rocking and torsional dynamic stiffnesses associated with the pile-soil parameters used in Figs. 2 and 3, respectively. Most of the observations on the characteristics of the horizontal and vertical stiffnesses apply to the rocking and torsional stiffnesses as well. Greater interaction effects for those cases are, however, associated with the in-phase vibration of piles.

An important characteristic that differentiates the behavior of pile groups from single piles is associated with the concept of pressure bulb. The pressure bulb is defined here as the zone in the neighborhood of the foundation where stresses (and strains) are significant. Consequently, the characteristics of this zone play a major role in the behavior of the foundation. Since this zone extends to depths which are comparable to the size of the foundation, one is led to expect that pile groups are influenced to a greater extent in their overall response by the characteristics of the deeper layers than single piles are, whose behavior is primarily controlled by the near-surface soil-pile properties. This can be verified, in fact, by examining the results in Fig. 6. This figure compares the ratio of the absolute values of the stiffnesses of a pile group, embedded in two different soil media: the first medium being a homogeneous halfspace with $E_s/E_p = 10^{-2}$, and the second, a halfspace similar to the former, but overlain by a surface layer with thickness $h = d$ and stiffness ratio $E_s/E_p = 10^{-3}$ (i.e., 10 times softer). This second case is intended to simulate (in an admittedly gross manner) the nonlinear effects that may be expected in the neighborhood of the pile heads as a result of soil yielding and pile-soil separation. The results clearly show that, as the number of piles increases, the stiffness ratio at low frequencies increases, and approaches unity. Hence, single piles are much more heavily influenced by conditions near the pile head than groups are. This has important design implications, especially when the results of field tests on single piles are used to infer group stiffnesses, since material and geometric nonlinearities near the surface considerably affect their behavior. Conversely, rigorous incremental solutions with nonlinear numerical models of single piles (or equivalent P-Y curves) cannot be used reliably to derive the group stiffness via empirical group factors.

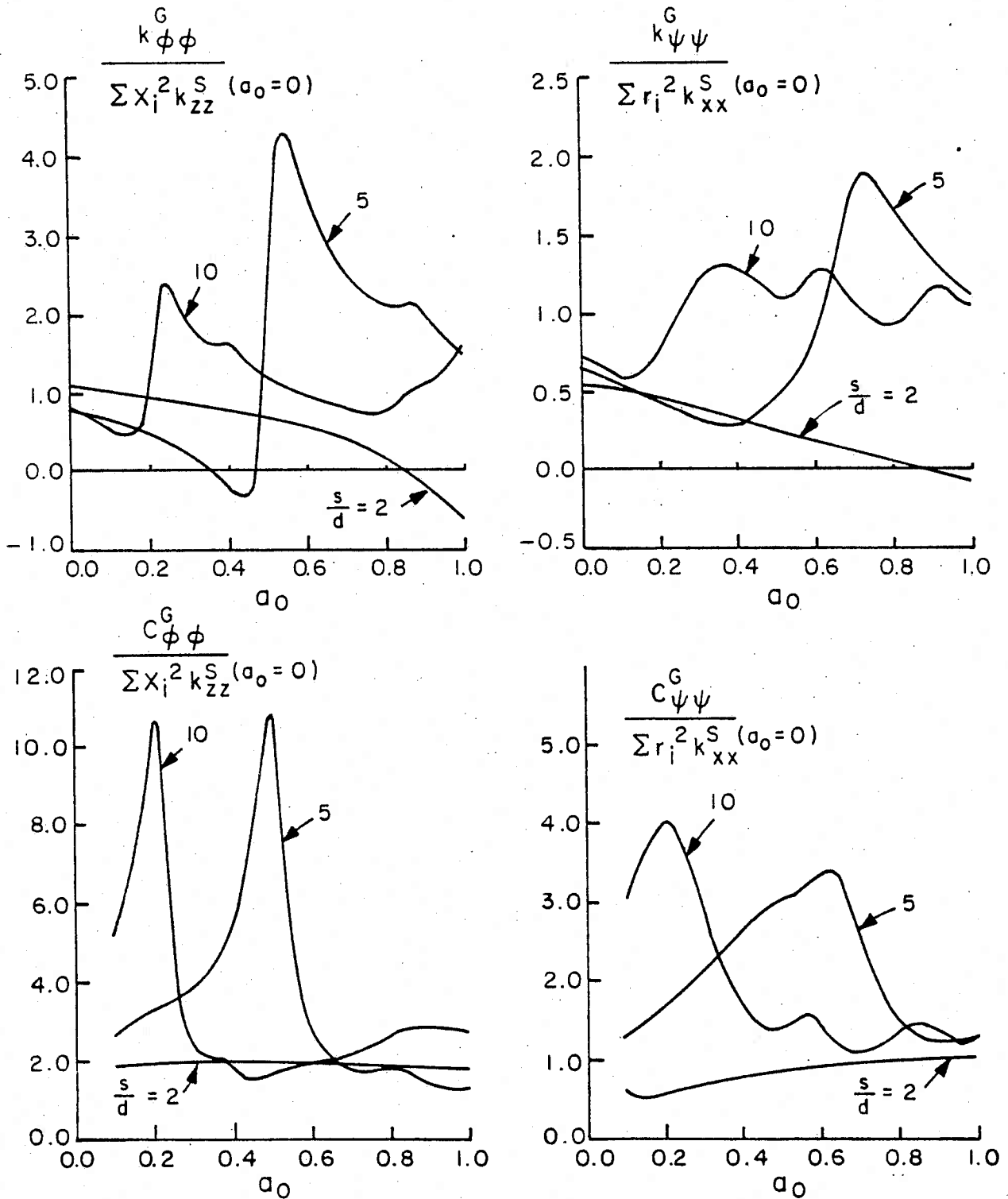$$\frac{L}{d} = 15; \quad \frac{E_s}{E_p} = 10^{-3}; \quad \frac{\rho_s}{\rho_p} = 0.70$$

Fig. 4 - Rocking and Torsional Dynamic Stiff-
nesses for 4 x 4 Pile Groups.

$$\frac{L}{d} = 15 \; ; \quad \frac{s}{d} = 5 \; ; \quad \frac{E_s}{E_p} = 10^{-2} \; ; \quad \frac{\rho_s}{\rho_p} = 0.70$$
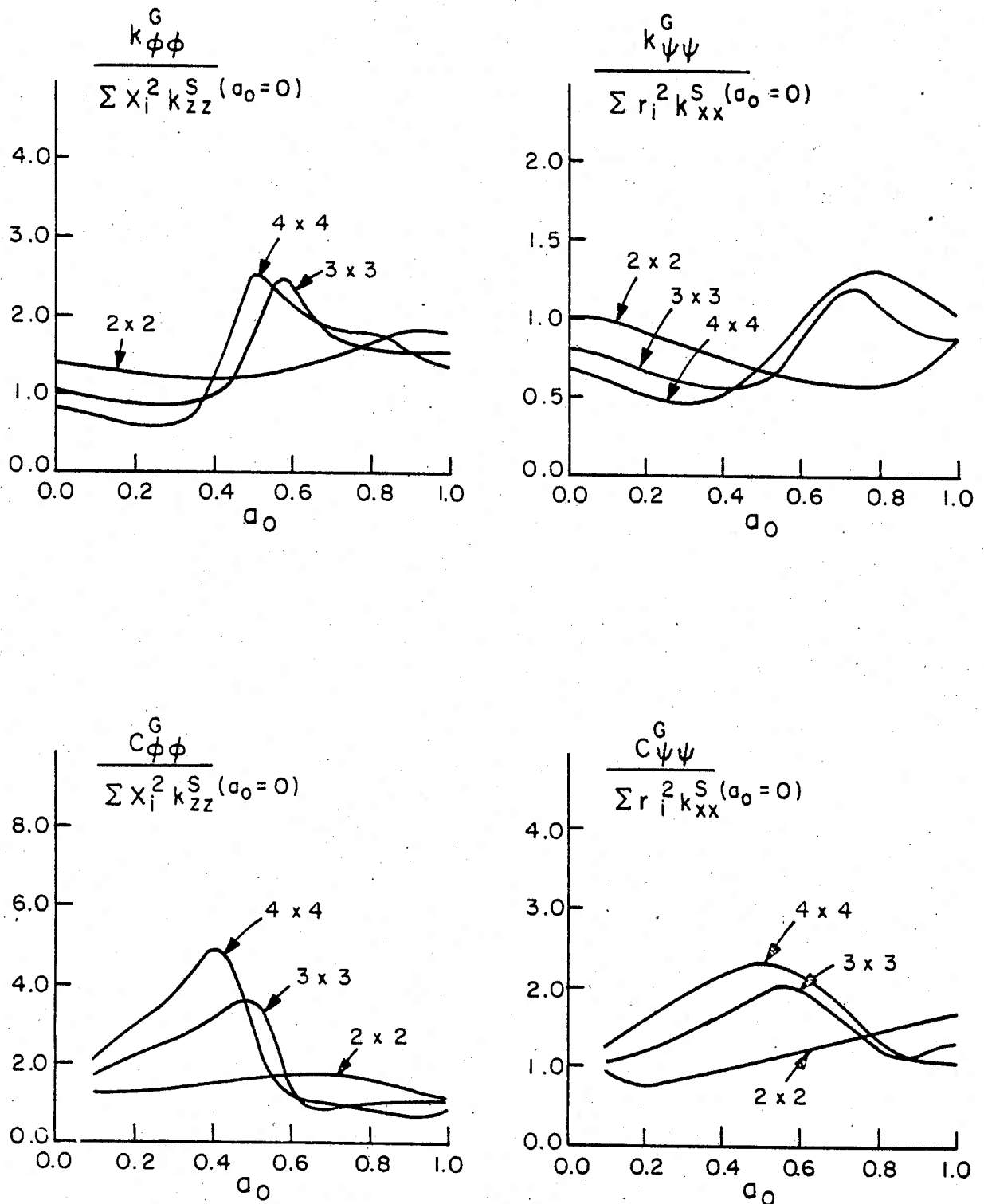

Fig. 5 – Rocking and Torsional Dynamic Stiffnesses
of Pile Groups with s/d = 5.

$$\frac{L}{d} = 15; \quad \frac{s}{d} = 5; \quad \frac{\rho_s}{\rho_p} = 0.70$$

$$1 - \text{LAYER SYSTEM: HALF SPACE;} \quad \frac{E_s}{E_p} = 10^{-2}$$

2 - LAYER SYSTEM: TOP LAYER: $\frac{h}{d} = 1; \quad \frac{E_s}{E_p} = 10^{-3}$

BOT. LAYER: HALF SPACE; $\frac{E_s}{E_p} = 10^{-2}$
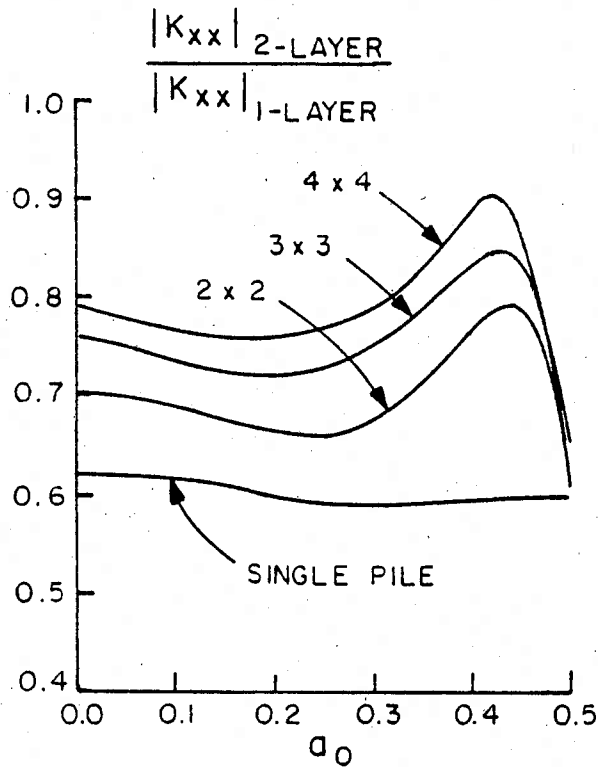
Fig. 6 - Ratio of Horizontal Pile Group Stiffness
for Two Different Soil Media.

b) Seismic response of pile groups.

Fig. 7 presents the seismic response of a 4 x 4 pile group, for which the stiffness characteristics were studied in Figs. 2 and 4. In these figures, $|u|$ is the absolute value of the horizontal displacement of the foundation caused by shear waves propagating vertically in the halfspace and producing a free-field ground-surface displacement u_g; and $|\phi|$ is the absolute value of the rotation of the foundation. Fig. 8 presents the corresponding quantities for the pile groups studied in Figs. 3 and 5. These figures display a significant dependence of $|\phi|$ on the width of the foundation.

On the other hand, for translation, the pile cap essentially follows the ground motion, although it filters out to some degree its high frequency components. For example, in Fig. 7, if C_s = 100 m/sec, d = 1 m, then a dimensionless frequency a_o = 0.2 corresponds to a physical frequency f = 3.18 Hz; since the filter function is essentially unity up to this frequency, and the earthquake will be characterized by low frequency components (soft soil!), it can be concluded that the motion of the pile cap and the soil will be very similar.

c) Distribution of forces on the pile raft among the piles.

Dynamic stiffnesses and seismic response analyses, as discussed above, play the principal role in the design of the superstructure. However, for the design of the piles themselves, one needs to know the distribution of forces among the piles. Examples of such distributions are presented in Fig. 9 for the same pile groups studied in Figs. 2 and 4. The first four plots in this figure show the absolute values of shear and moment at pile-head level caused by a shearing force applied on the foundation. The results are normalized with respect to the shear that would be observed in each pile if there were no interaction effects (i.e., total shear/N). The remaining plots in Fig. 9 correspond to the axial forces observed at pile-head level, caused by a vertical force on the foundation, again normalized with respect to the average vertical force. These figures show that for the static case, the corner piles carry the largest portion of the load, while the piles closest to the center carry the smallest. However, this observation is no longer valid in the dynamic case. In fact, for some frequencies, a load distribution

14

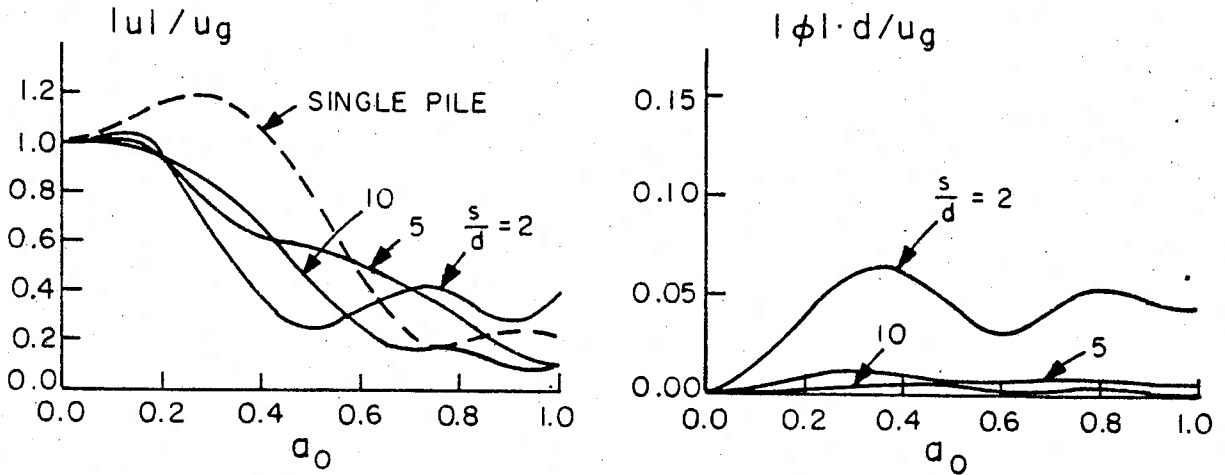$$\frac{L}{d} = 15 \; ; \quad \frac{E_s}{E_p} = 10^{-3} \; ; \quad \frac{\rho_s}{\rho_p} = 0.70$$

Fig. 7 - Absolute Value of Transfer Functions for Horizontal Displacement and Rotation of the Pile Cap for 4 x 4 Pile Groups.

$$\frac{L}{d} = 15 \; ; \quad \frac{E_s}{E_p} = 10^{-2} \; ; \quad \frac{\rho_s}{\rho_p} = 0.70$$
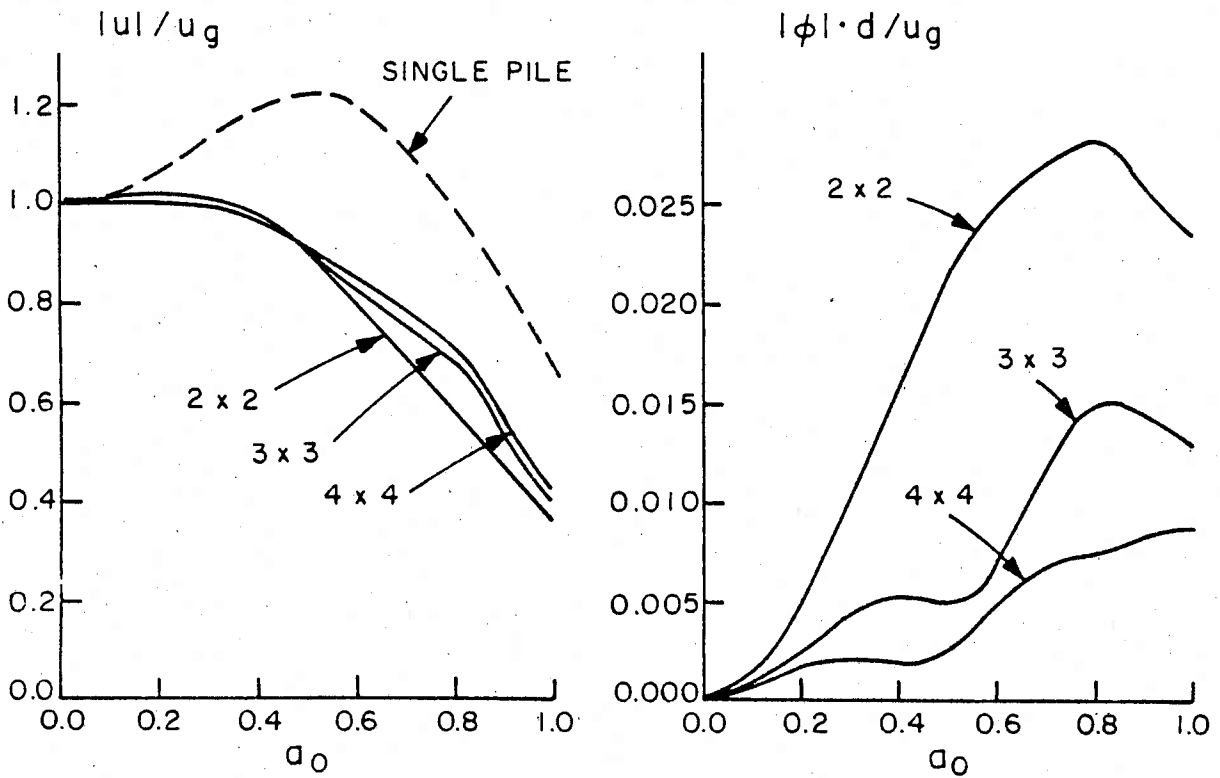

Fig. 8 - Absolute Value of Transfer Functions for Horizontal Displacement and Rotation of the Pile Cap for s/d = 5.

$$\frac{L}{d} = 15; \quad \frac{E_s}{E_p} = 10^{-3}; \quad \frac{\rho_s}{\rho_p} = 0.70$$

$$\begin{cases} \overline{R}_x = |R_x| \, / \, \text{AVG. SHEAR} \\ \overline{M}_x = |M_x| \, / \, dx \, (\text{AVG. SHEAR}) \end{cases} \quad \overline{R}_z = |R_z| \, / \, \text{AVG. AXIAL FORCE}$$
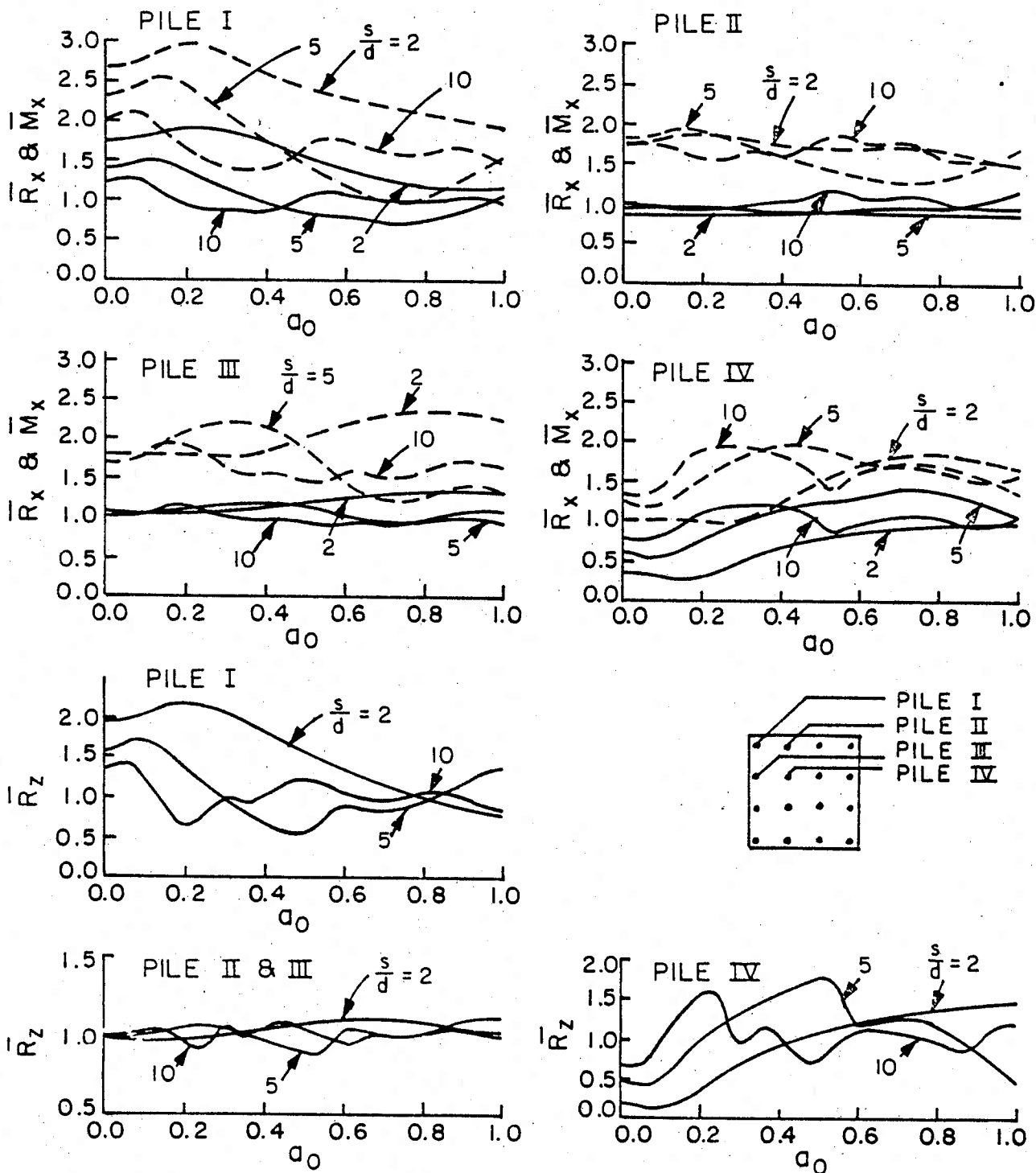
Fig. 9 - Distribution of Horizontal and Vertical Forces on the Pile Cap among the Piles.

favorable to corner piles may take place. This can be verified, for instance, by examining the variation with frequency of the axial force on piles I and IV for $s/d = 2$. Observe also the considerable dynamic amplification of the pile forces for some frequencies, which is as large as 5 on pile IV for $s/d = 2$.

The superposition method

The superposition method originally proposed by Poulos (7,8) is frequently used to formulate pile group problems. In this approximate scheme, only two piles are considered at a time in the formation of the global flexibility matrix. The entries in this matrix are obtained from tabulated solutions for two piles that are commonly referred to as interaction factors, and which are presented in terms of the distance separating the piles, and the material properties of the system. The foundation stiffnesses for the whole group are then obtained in a manner similar to that outlined earlier in this paper.

The available tabulated solutions for the interaction factors are for static loads only. To extend the applicability of the method to dynamic loads it is necessary to develop appropriate factors for this purpose. Graphs for these factors are presented in Figs. 10 and 11 for the pile-soil types considered earlier in this paper.

A dynamic interaction factor for two piles (in which the first is loaded with a unit harmonic load, and the displacements are observed on the second) is defined as follows:
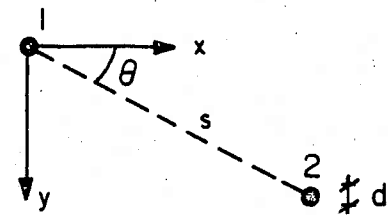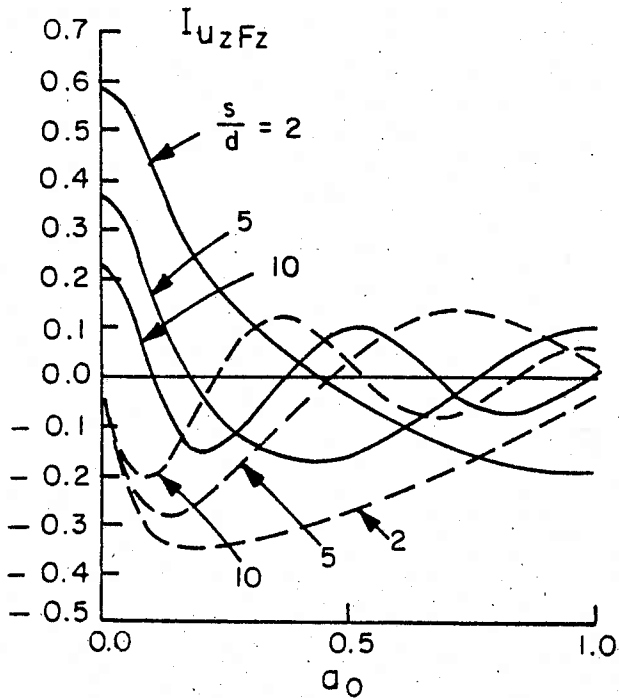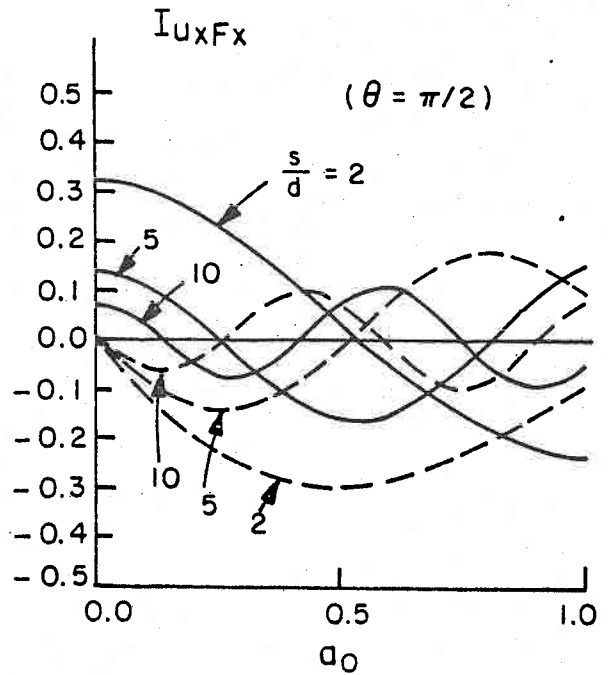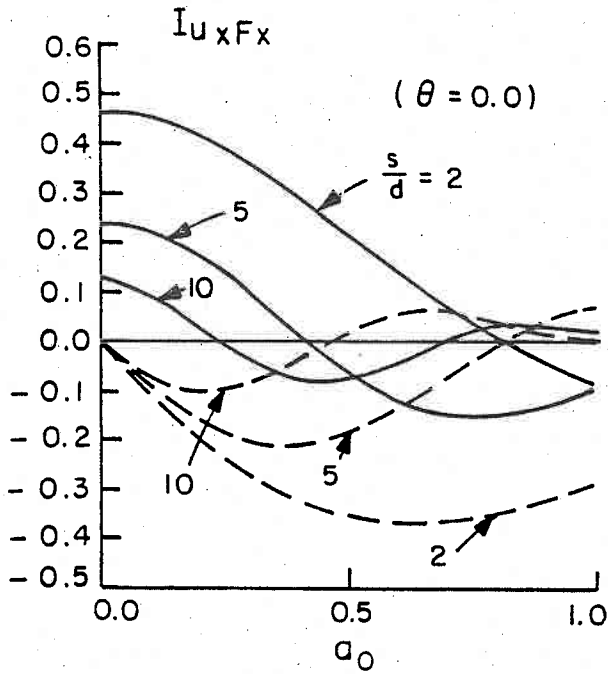
$$\text{Interaction factor} = \frac{\text{Dynamic displ. of pile 2}}{\text{Static displ. of pile 1, considered individually}}$$

in which the word displacement stands for either a translation or a rotation. The method is based on the observation that

$$\frac{\text{Displ. of pile 1}}{\text{Displ. of pile 1, considered individually}} \approx 1$$

That is, the second pile hardly affects the displacements of the loaded pile. Application of the method requires also the dynamic load factors for individually loaded piles (single piles), which are available in the literature.

$$\frac{L}{d} = 15 \; ; \quad \frac{E_s}{E_p} = 10^{-3} \; ; \quad \frac{\rho_s}{\rho_p} = 0.70$$
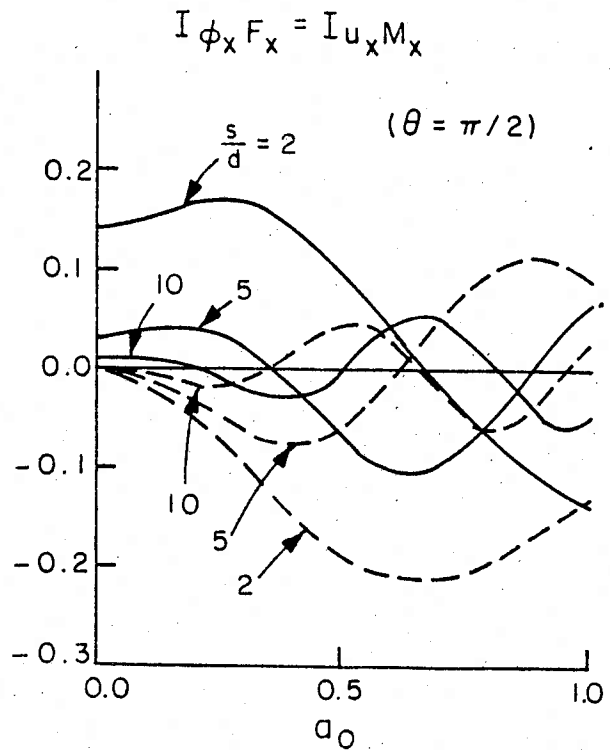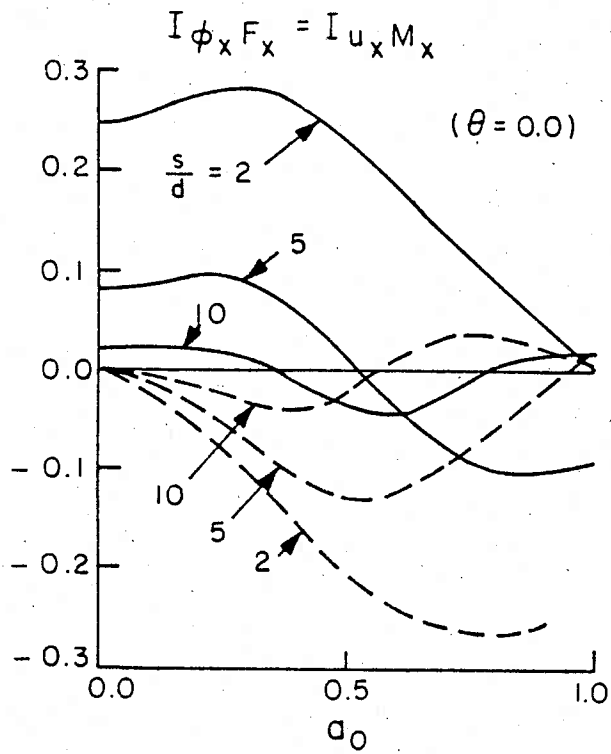

Fig. 10 - Interaction Curves for Horizontal and Vertical Displacement of Pile 2 Due to Horizontal and Vertical Force on Pile 1.

18

$$\frac{L}{d} = 15; \quad \frac{E_s}{E_p} = 10^{-3}; \quad \frac{\rho_s}{\rho_p} = 0.70$$

$I_{\phi_x F_x} = I_{u_x M_x}$ ($\theta = 0.0$)

$I_{\phi_x F_x} = I_{u_x M_x}$ ($\theta = \pi/2$)

——— Real Part ——— Imag. Part

$I_{\phi_x M_x}$ ($\theta = 0.0$)

$I_{\phi_x M_x}$ ($\theta = \pi/2$)
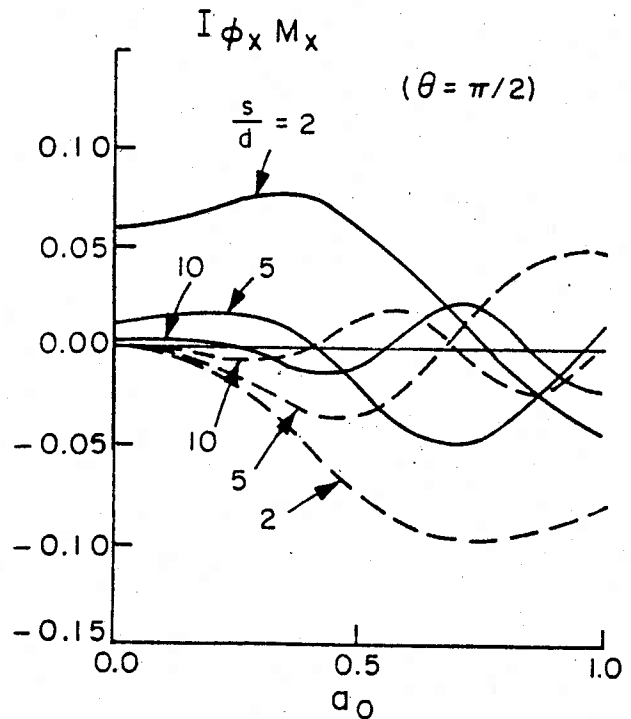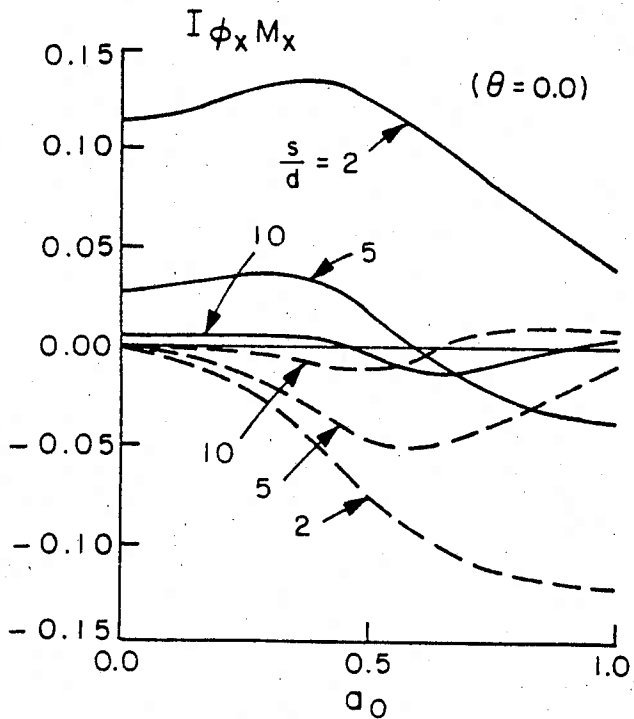
$I_{\phi_x F_x} \equiv$ rotation of pile 2 due to horizontal force on pile 1.

$I_{\phi_x M_x} \equiv$ rotation of pile 2 due to moment on pile 1.

Fig. 11 – Interaction Curves for Rotation of Pile 2 Due to Horizontal Force and Moment on Pile 1.

The dynamic interaction curves are also helpful in gaining insight into the behavior of pile groups. For example, examination of Figs. 2 and 10, for $s/d = 5$, vertical case, shows a large peak in k_{zz} (Fig. 2) occurring at a frequency $a_o \approx 0.45$ for which the interaction factor is a real, negative number (Fig. 10). Physically, this means that the waves set up by the loaded pile excite the second pile in an antiphase motion; thus, a larger force (stiffness) must be applied on each pile to enforce the condition of uniform displacement of the pile heads required by the presence of the pile cap. A similar argument concerning the frequencies for which equiphase motion occurs can be brought forward to explain valleys in the stiffness functions.

Figures 12 and 13 display the dynamic stiffnesses for the same pile groups of Figs. 2 and 4, but computed using the superposition method. Comparison of these figures shows that the approximate superposition method yields results that are in good general agreement with those obtained from the full three-dimensional analysis enforcing compatibility between all the piles in the group. The accuracy of the approximation improves as the pile spacing is increased, as expected.

Conclusion

The results provided by this study suggest the following observations:

a) The dynamic behavior is highly dependent on frequency, as a result of constructive or destructive interference taking place between the various piles in the group. Radiation damping generally increases with foundation size.

b) Pile groups subjected to seismic excitations essentially follow the low frequency components of the ground motion, while filtering to an important degree its intermediate and high frequency components. The rotational component, on the other hand, is negligibly small for typical dimensions of the foundation.

c) Forces on the piles generally increase towards the edge of the raft, except for some frequencies. Also, large dynamic amplification factors for these forces may be expected.

$$\frac{L}{d} = 15 \; ; \quad \frac{E_s}{E_p} = 10^{-3} \; ; \quad \frac{\rho_s}{\rho_p} = 0.70$$
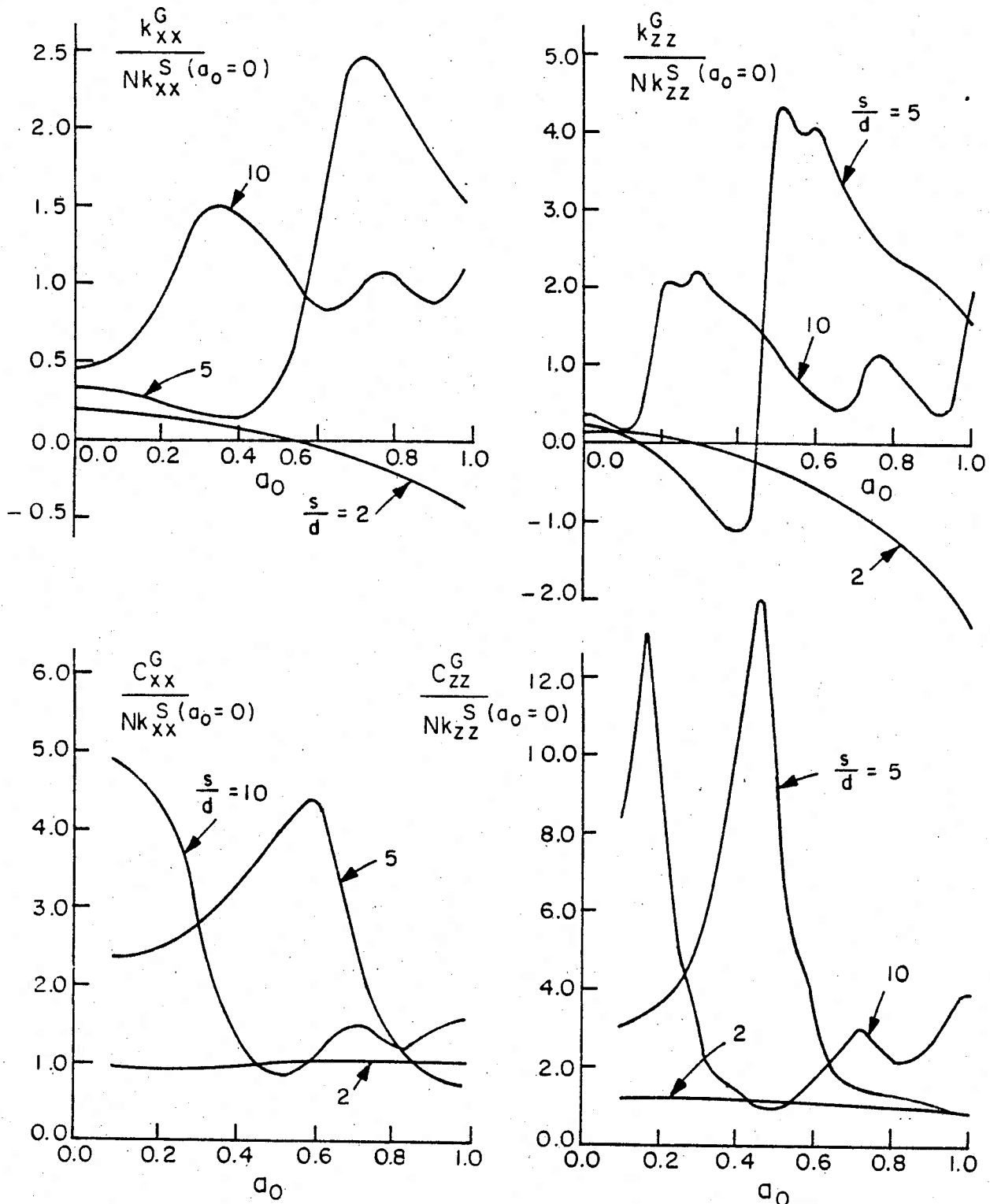

Fig. 12 - Horizontal and Vertical Dynamic Stiffnesses for 4 x 4 Pile Groups by the Superposition Technique.

$$\frac{L}{d} = 15 \; ; \quad \frac{E_s}{E_p} = 10^{-3} \; ; \quad \frac{\rho_s}{\rho_p} = 0.70$$
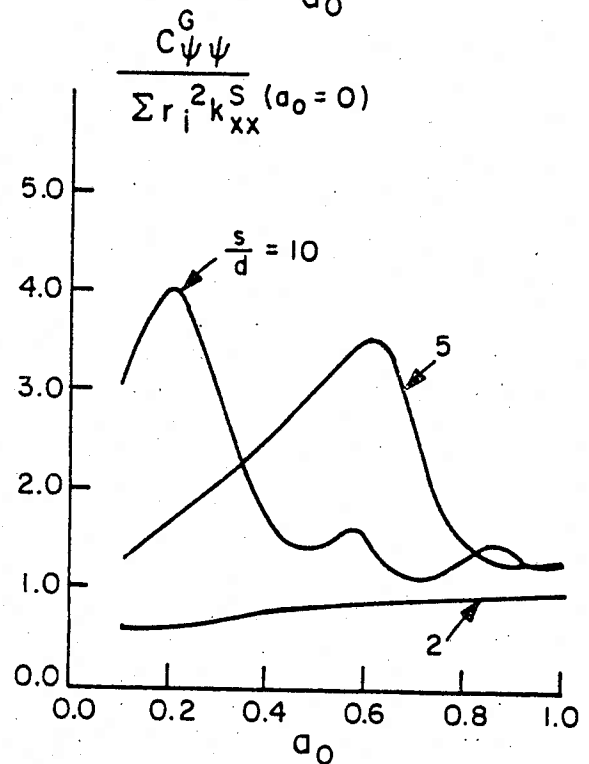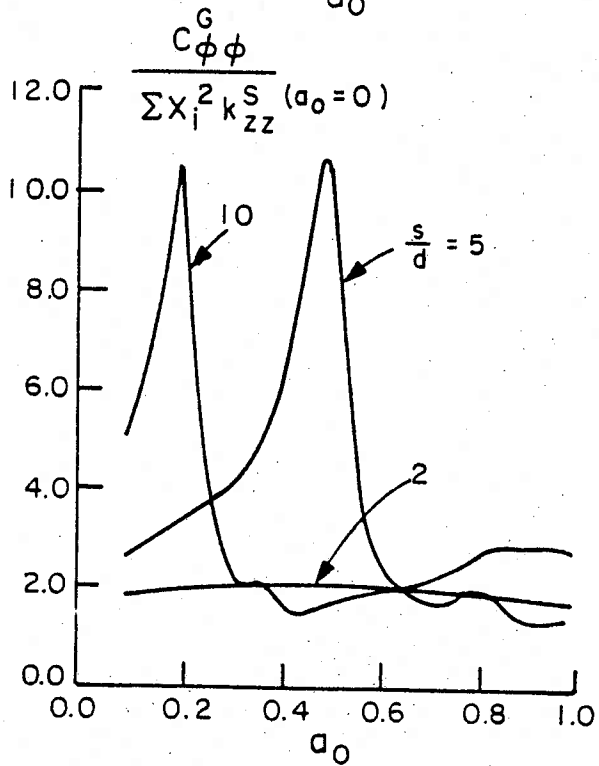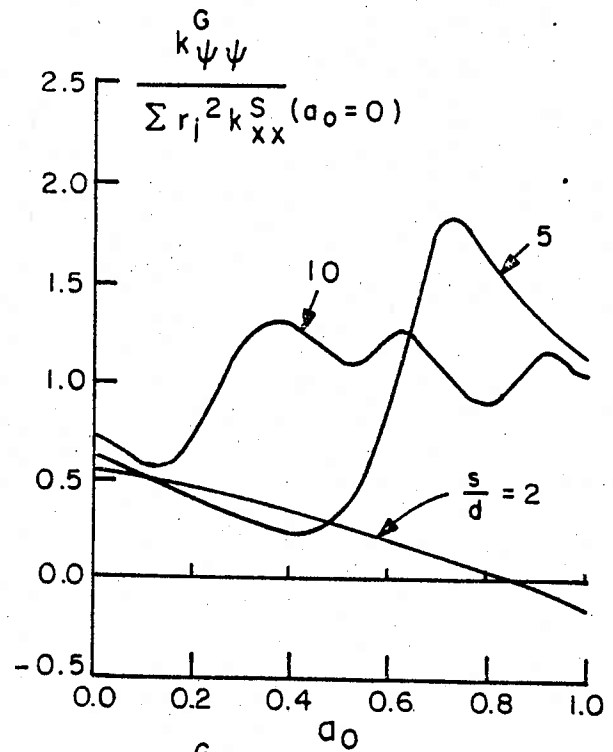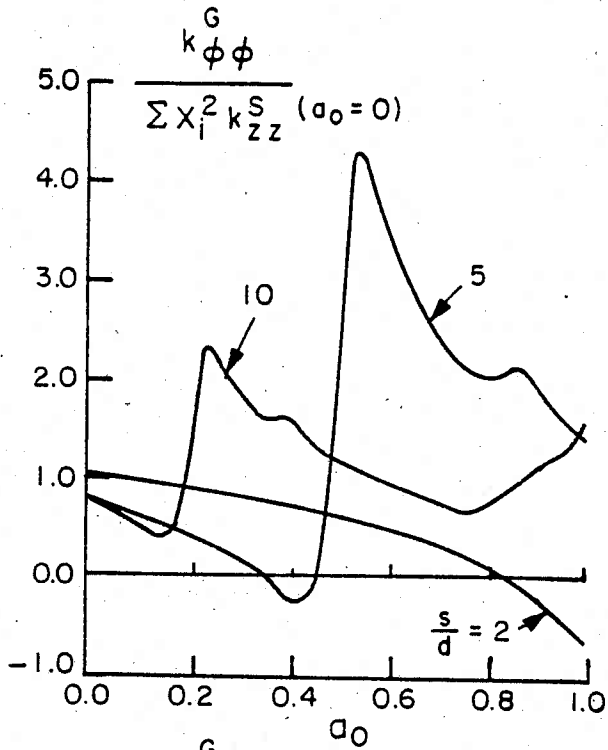

Fig. 13 - Rocking and Torsional Dynamic Stiffnesses for 4 x 4 Pile Groups by the Superposition Technique.

d) Nonlinear solutions (or P-Y curves) for single piles cannot reliably be used to assess group stiffnesses in combination with group factors.

e) Field tests on single piles may be poor predictors of group behavior.

f) The superposition scheme suggested first by Poulos gives reasonable results not only for static loads, but for dynamic ones as well.

ACKNOWLEDGEMENT

References

1. Apsel, R., "Dynamic Green's Functions for Layered Media and Applications to Boundary-value Problems," Ph.D. Thesis submitted to the Department of Applied Mechanics and Engineering Sciences, University of California, San Diego, 1979.

2. Banerjee, P.K., "Analysis of Axially and Laterally Loaded Pile Groups, in Developments in Soil Mechanics, Ed., C.E. Scott, Chapter 9, Applied Science Publishers, London, 1978.

3. Banerjee, P.K. and Driscoll, P.M., "Three-dimensional Analysis of Raked Pile Groups," Proc. Instn. Civ. Engrs., Part 2, Vol. 61: 643-671, 1978.

4. Kaynia, A.M., "Dynamic Stiffnesses and Seismic Response of Pile Groups," Ph.D. Thesis submitted to the Department of Civil Engineering, Massachusetts Institute of Technology, January 1982.

5. Nogami, T., "Dynamic Group Effect of Multiple Piles under Vertical Vibration," Proc. of ASCE Engineering Mechanics Specialty Conference, Austin, Texas, 1979.

6. Nogami, T., "Dynamic Stiffnesses and Damping of Pile Groups in Inhomogeneous Soil," ASCE special technical publication on Dynamic Response of Pile Foundations, October 1980.

7. Poulos, H.G., "Analysis of the Settlement of Pile Groups," Geotechnique, Vol. 18, 1968, pp. 449-471.

8. Poulos, H.G., "Behavior of Laterally-Loaded Piles: II-Pile Groups," Journal of the Soil Mechanics and Foundation Division, ASCE, Vol. 97, No. SM5, 1971, pp. 733-751.

9. Poulos, H.G. and Davis, E.H., "Pile Foundation Analysis and Design," John Wiley and Sons, New York, N.Y., 1980.

10. Waas, G. and Hartmann, H.G., "Analysis of Pile Foundations under Dynamic Loads," SMIRT Conference, Paris, 1981.

11. Wolf, J.P. and Von Arx, G.A., "Impedance Function of A Group of Vertical Piles," Proc. of the ASCE Geotechnical Engineering Division, Specialty Conference on Earthquake Engineering and Soil Dynamics," Pasadena, California, 1978, pp. 1024-1041.